1 **Bacteriophage ΦM1 of *Pectobacterium* evolves to escape two bifunctional Type III**

2 **toxin-antitoxin and abortive infection systems through mutations in a single viral**

3 **gene**

4

5 **Authors:** Tim R. Blower[1*], Ray Chai[1], Rita Przybilski[2], Shahzad Chindhy[1], Xinzhe Fang[1],

6 Samuel E. Kidman[1], Hui Tan[1], Ben F. Luisi[1], Peter C. Fineran[2] and George P. C. Salmond[1#].

7 *[1]Department of Biochemistry, University of Cambridge, Cambridge, CB2 1QW, United*

8 *Kingdom; [2]Department of Microbiology and Immunology, University of Otago, P.O. Box 56,*

9 *Dunedin 9054, New Zealand.*

10 *[*]Current address: Department of Biosciences, Durham University, South Road, Durham, DH1*

11 *3LE*

12

13 Running head: **ΦM1 escapes two Type III TA systems by the same route**

14 **Key words:** Type III toxin-antitoxin, ΦM1, *Pectobacterium atrosepticum*, abortive

15 infection, bacteriophage-bacteria interaction

16

17 #Correspondence should be addressed to George P.C. Salmond at Department of Biochemistry,

18 University of Cambridge, Cambridge, CB2 1QW, United Kingdom. Email: gpcs2@cam.ac.uk.

19 Tel. +44(0)1223 333650.

20

ABSTRACT

Some bacteria, when infected by their viral parasites (bacteriophages), undergo a suicidal response that also terminates productive viral replication (abortive infection; Abi). This response can be viewed as an altruistic act protecting the uninfected bacterial clonal population. Abortive infection can occur through the action of Type III protein-RNA toxin-antitoxin (TA) systems, such as ToxIN$_{Pa}$ from the phytopathogen, *Pectobacterium atrosepticum*. Rare spontaneous mutants evolved in the generalized transducing phage, ΦM1, which escaped ToxIN$_{Pa}$-mediated abortive infection in *P. atrosepticum*. ΦM1 is a member of the *Podoviridae* and member of the "KMV-like viruses", a subset of the T7 supergroup. Genomic sequencing of ΦM1 escape mutants revealed single-base changes which clustered in a single open reading frame. The "escape" gene product, M1-23, was highly toxic to the host bacterium when over-expressed, but mutations in M1-23 that enabled an escape phenotype caused M1-23 to be less toxic. M1-23 is encoded within the DNA metabolism modular section of the phage genome, and when it was over-expressed, it co-purified with the host nucleotide excision repair protein, UvrA. While the M1-23 protein interacted with UvrA in co-immunoprecipitation assays, a UvrA mutant strain still aborted ΦM1, suggesting that the interaction is not critical for the Type III TA Abi activity. Additionally, ΦM1 escaped a heterologous Type III TA system (TenpIN$_{Pl}$) from *Photorhabdus luminescens* (reconstituted in *P. atrosepticum*) through mutations in the same protein, M1-23. The mechanistic action of M1-23 is currently unknown but further analysis of this protein could provide insights into the mode of activation of both systems.

IMPORTANCE

Bacteriophages, the viral predators of bacteria, are the most abundant biological entities and are important factors in driving bacterial evolution. In order to survive infection by these viruses, bacteria have evolved numerous anti-phage mechanisms. Many of the studies involved in understanding these interactions have led to the discovery of biotechnological and gene-editing tools, most notably restriction enzymes and more recently the CRISPR-Cas systems. Abortive infection is another such anti-phage mechanism that warrants further investigation. It is unique in that activation of the system leads to the premature death of the infected cells. As bacteria infected with the virus are destined to die, undergoing precocious suicide prevents the release of progeny phage and protects the rest of the bacterial population. This altruistic suicide can be caused by Type III toxin-antitoxin systems and understanding the activation mechanisms involved will provide deeper insight into the abortive infection process.

INTRODUCTION

It is estimated that there are more than 10^{30} bacteriophages (phages) on Earth, outnumbering their bacterial hosts tenfold (1, 2). These large viral numbers generate an estimated 10^{25} infections per second, imposing a large evolutionary selection pressure on bacteria (2). In response, bacteria have evolved a plethora of defensive mechanisms to counter these overwhelming phage insults (3). Consequently, phages are continually evolving counter defences and thus both the host and parasite are locked together in a perpetual molecular arms race (4). Bacterial anti-phage mechanisms that have been observed include adsorption prevention, restriction-modification systems, superinfection systems, abortive infection (Abi) systems and the clustered regularly interspaced short palindromic repeats (CRISPR)-Cas systems (3). Studies of these phage-host interactions have been translated into significant molecular technologies and reagents, most notably the use of restriction enzymes in cloning (5) and, more recently the CRISPR-Cas systems use of which is currently revolutionising eukaryotic molecular biology (6).

One of the more curious anti-phage mechanisms is Abi where, post-infection, the host bacterium is driven towards precocious cell death. This simultaneously terminates viral replication and prevents a productive phage burst. Thus, the Abi response in infected cells protects the bacterial population from progeny phage infection in a process akin to an altruistic suicide (3). The majority of Abi systems have been studied in *Lactococcus lactis* (7), an important bacterium in the dairy industry (8). Phage contamination in fermentation cultures can cause substantial economic losses. Consequently, considerable research has been conducted to identify and define many anti-phage systems useful for control of bacteriophages in lactococcal fermentations (7). However, there are also well-studied Abi systems in other bacteria such as *Escherichia coli*, namely the Rex, Lit and PrrC systems (9-11). A commonly recurring theme of

76   Abi systems is that they involve the activation of a toxic protein that is suppressed under normal

77   growth conditions. However, environmental insults, phages, or other physiological stresses can

78   activate the toxin. Once activated, the toxin interferes with an essential cellular process and

79   induces bacteriostasis, ultimately leading to cell death. This is a common feature shared by toxin-

80   antitoxin systems (12).

81   Toxin-antitoxin (TA) systems were originally discovered on plasmids where they

82   function as plasmid maintenance systems through post-segregational killing mechanisms (13).

83   They have been found in the majority of bacteria, both on plasmids (13) and chromosomally

84   (14), as well as in archaea (15) and phages (16). TA systems are typically bicistronic, comprising

85   a bacteriostatic or bactericidal toxic protein that is neutralized either directly or indirectly by an

86   antitoxin counterpart. To date there are six TA system Types which are characterized by the

87   nature and mode of action of their antitoxins (17). In the case of Type III TA systems, an RNA

88   antitoxin directly interacts with the toxic protein to form a non-toxic complex (18).

89   At least four Types of TA systems confer phage resistance. These are the *hok/sok* systems

90   of Type I (19), *mazEF*, *rnlAB* and *lsoAB* of Type II (20, 21), ToxIN$_{Pa}$, TenpIN$_{Pl}$ and AbiQ of

91   Type III (22-24), AbiE of Type IV (25) and sanaTA (which is currently not characterized but

92   likely to be a Type II, having a proteinaceous antitoxin) (26). ToxIN$_{Pa}$ was the first Type III

93   system to be identified and originated from *Pectobacterium atrosepticum* plasmid pECA1039.

94   The toxin ToxN$_{Pa}$ is encoded by *toxN* and the antitoxin ToxI$_{Pa}$ is encoded by *toxI*, a 36 nucleotide

95   sequence repeated five and a half times (22). The ToxIN$_{Pa}$ system provides protection against

96   multiple phages infecting not only its cognate host, *P. atrosepticum,* but also other enteric

97   bacteria including *E. coli* DH5α and *Serratia marcescens* Db11 (22). One such aborted

98   pectobacterial phage is the *Myoviridae* phage, ΦTE. ΦTE phages that were no longer sensitive to

5

99   ToxIN$_{Pa}$ had evolved to encode an RNA antitoxic mimic of ToxI$_{Pa}$, which was able to neutralize

100 ToxN$_{Pa}$ (27). However, it did not shed light on how ToxIN$_{Pa}$ was activated during phage

101 infection. In fact, very little is known about the activation of any Type III toxin-antitoxin

102 systems. The other Type III system that has been studied for Abi is AbiQ from *Lactococcus*

103 *lactis*, which shows structural homology with ToxN$_{Pa}$ (24). Three lactococcal siphophages that

104 were aborted by AbiQ have been examined in detail. However, all had mutations in genes of

105 unknown functions; *orf38*, *m1* and *e19* of phages P008, bIL170 and c2, respectively (28). The

106 AbiQ system was also reconstructed in a heterologous host, *E. coli* MG1655, and was shown to

107 confer resistance to a range of coliphages including T4 and T5. However, escape mutants could

108 only be obtained for a single phage (Phage 2). Escapes of this phage showed mutations in *orf210*,

109 a predicted DNA polymerase (28). Studies of the AbiQ system suggests there may be multiple

110 potential routes of escape involving several genes from different phages in the activation of a

111 single Abi system.

112   Previously it was shown that the pectobacterial phage, ΦM1, was aborted by the ToxIN$_{Pa}$

113 system and was able to escape by evolving rare mutants (29). ΦM1 was isolated in 1995 during a

114 search for new transducing phages effective as genetic tools in *P. atrosepticum* (30). Here we

115 characterize ΦM1 and its escape mutants in depth. All ΦM1 escape phages evolved through

116 mutations in a gene encoding a small highly toxic protein, M1-23. When the related TenpIN$_{Pl}$

117 system of *Photorhabdus luminescens* was transferred to *P. atrosepticum*, the system was able to

118 abort ΦM1 in the heterologous host. Furthermore, it was possible to select spontaneous viral

119 mutants that escaped both ToxIN$_{Pa}$ and TenpIN$_{Pl}$ through mutations in M1-23.

120

121

6

MATERIALS AND METHODS

Bacterial strains, bacteriophages and growth conditions

Bacterial strains and bacteriophages are listed in Table 1. *E. coli* strains were grown at 37°C and *Pectobacterium atrosepticum* SCRI1043 (Pba) (31) was grown either at 25°C on agar plates or at 25, 28, or 30°C as required for liquid culture, in Luria broth (LB) at 250 rpm or on LB-agar (LBA). LBA contained 1.5% w v^{-1} or 0.35% w v^{-1} agar, to make LBA plates or top-LBA, respectively. Bacterial growth was measured using a spectrophotometer set to 600 nm. When required, media were supplemented with ampicillin (Ap) at 100 μg ml^{-1}, chloramphenicol (Cm) at 50 μg ml^{-1}, kanamycin (Km) at 50 μg ml^{-1} tetracycline (Tc) at 10 μg ml^{-1}, Isopropyl β-D-thiogalactopyranoside (IPTG) at 0.5 mM or 2, 6-diaminopimelic acid (DAPA) at 300 μM. Phage spontaneous escape mutants were isolated as described previously (27). Phage lysates were made as described (32). Phages were stored at 4°C in phage buffer; 10 mM Tris-HCl pH 7.4, 10 mM MgSO$_4$, 0.01% w v^{-1} gelatin. A few drops of chloroform saturated with sodium bicarbonate was also added to the phage lysates to maintain sterility. Efficiency of Plating (EOP) was calculated after overnight incubation of serial dilutions of phage lysates in a top-LBA lawn of each bacterial host, and recorded as plaque forming units (pfu) on test strain/pfu on control strain. EOPs were calculated using Pba wild type (wt) or a frame-shifted *toxN* plasmid strain as the negative control (22).

ΦM1 genomic sequencing

Bacteriophage DNA was extracted with phenol/chloroform, using phase-lock gel tubes (Eppendorf) and following the manufacturer's instructions, as for bacteriophage λ. The extracted DNA was subjected to pyrosequencing on a Roche 454 Genome Sequencer FLX at the DNA

7

145 sequencing facility, Department of Biochemistry, University of Cambridge. Contiguous read

146 segments (contigs) were assembled using Newbler (Roche). The ΦM1 wild type sequence was

147 determined in one lane of the sequencing run. The three escape phage genomes were individually

148 tagged with independent identifying sequences, then combined and sequenced as a mixture

149 within a second lane. For each of the four phages, the final assembled sequence consisted of a

150 single contig of approximately 43,500 base-pairs (bp). The average read length was 250 bp. The

151 wild type sequence was assembled from 13,628 reads, leading to approximately 78x coverage of

152 the full sequence. Escape phage ΦM1-A, -B and -D sequences were assembled from 4925, 5188

153 and 5886 reads, respectively, resulting in approximately 29x coverage of each sequence.

154   When viewing the sequence data, beginning at 43,572 bp (in the final ΦM1 wt sequence),

155 there were fifteen tandem repeats of the 2 bp sequence 'TG'. The number of TG repeats varied

156 between the raw sequences of each phage, from seventeen in ΦM1-A to one in ΦM1-B and

157 seven in ΦM1-D. The exact number of TG repeats in each phage genome could not be accurately

158 confirmed by sequencing a specific amplicon. Therefore, in order to sequence this region, it was

159 specifically amplified (Primers TRB107/108 and TRB115/116) and cloned into pBR322 (NEB).

160 From the resulting plasmid DNA, the region was successfully sequenced on both forward and

161 reverse strands.

162   Potential ORFs were identified using gene prediction tools such as ORFfinder

163 (http://www.ncbi.nlm.nih.gov/projects/gorf/), GeneMark.hmm (33) and Glimmer (34), along

164 with BLAST (35) homology searches and manual annotation. RBSfinder (36) was used to

165 predict ribosome-binding sites (Table S1). ΦM1 tRNAs were identified using tRNAScan-SE

166 (37). The BDGP Neural Network Promoter Prediction (38) program did not identify any

167 consensus promoters. The program, "Stretcher", from the EMBOSS suite

168   (http://www.ebi.ac.uk/Tools/psa/emboss_stretcher/nucleotide.html), was used for global

169   nucleotide alignments. The ΦM1 genome was viewed and annotated using Artemis (39).

170

171   **Plasmid construction**

172   Molecular biology techniques were performed as described previously (40). All primers were

173   obtained from Sigma-Genosys and Invitrogen and are listed in Table 2. All plasmids constructed

174   and/or used in this study are listed in Table 3, along with the primers used for their construction.

175   All recombinant plasmid sequences were verified by DNA sequencing.

176

177   **Measuring ToxI$_{Pa}$ and ToxN$_{Pa}$ Levels during Phage Infection**

178   Two cultures of 180 ml LB containing Ap were inoculated with 2 ml overnight cultures of Pba

179   (pBR322) or Pba (pMJ4), respectively. Cultures were grown at 25°C and shaken at 180 rpm to

180   an OD_{600} of 1 and each split into 2× 80 ml; one of which was infected with phage at a

181   multiplicity of infection (MOI) of 1, while the other served as a negative control without

182   infection. Cultures were left for 10 min without shaking for phage adsorption, then shaken at

183   25°C and 180 rpm. Samples for OD_{600} measurement, RNA preparation and protein analysis were

184   taken regularly during infection. Total RNA was isolated using the TRIZOL method and

185   subsequently DNase treated. Cell pellets for Western blot analysis were resuspended in 1× PBS

186   according to OD_{600} measurement.

187

188   **Western blot analysis of ToxN$_{Pa}$ during infection**

189   One ml samples of the cell cultures were taken, pelleted and resuspended in 1× PBS according to

190   OD_{600}. For samples taken during ΦM1 phage infection, the protein was quantified using a

9

191 Nanodrop (ThermoScientific) and equal amounts of protein (150 μg) were resolved by 12%

192 PAGE. Proteins were transferred to a PVDF-membrane and blocked for 1 h in 1× PBS

193 containing 5% milk powder. Immunodetection of FLAG-tagged ToxN was performed overnight

194 at 4°C in 1× PBS using anti-FLAG M2 antibody (Sigma). Goat anti-mouse IgG-HRP (Santa

195 Cruz) was used as secondary antibody. Bands were visualized on X-Ray film using the

196 SuperSignal West Pico Chemiluminescent Substrate Kit (Pierce). SdhE-FLAG expressed from

197 pMAT7 (41), was used as a control in the blot tracking ΦM1 infection.

198

S1-nuclease Protection Assays

200 An antisense probe covering the complete ToxI$_{Pa}$ sequence was made by amplification of the

201 ToxI$_{Pa}$ locus from plasmid pTA110, using primers PF217 and PF218, and subsequent *in vitro*

202 transcription and gel extraction of the probe as described (42), generating a uniformly ^{32}P-UTP

203 labeled antisense transcript. Ten μg of DNase-treated total RNA was hybridized to the antisense

204 probe overnight at 68°C in a total volume of 30 μl containing 22% or 6% formamide for the

205 ΦM1 and ΦM1-O total RNA, respectively, 40 mM PIPES/KOH (pH 6.4), 1 mM EDTA and 400

206 mM NaCl. Reactions were treated with S1-nuclease (Invitrogen) (1 U μl^{-1}) for 1.5 h at 37°C in a

207 total volume of 300 μl 1× S1-nuclease buffer, to degrade any single-stranded nucleic acids.

208 Double-stranded hybridization products were precipitated, resuspended and resolved by 10%

209 PAGE. Bands were visualized by phosphorimaging (BioRad Personal FX phosphorimager).

210

211

10

Toxicity assays

When required, media were supplemented with Ap, D-glucose (glu) at 0.2% w v^{-1} and L-arabinose (L-ara) at 0.1% w v^{-1}. Pba strains containing two plasmids were grown as 10 ml overnight cultures, then used to inoculate 25 ml LB, Ap, Cm and glu in 250 ml conical flasks, and grown at 25°C and 250 rpm, from a starting OD$_{600}$ of ~0.04, until exponential phase (~1 x 10^8 colony forming units (cfu) ml^{-1}). Samples were removed, washed with phosphate buffered saline (PBS), serially diluted and plated for viable counts at 25°C on LBA, Ap, Cm plates containing either i) glu, to repress expression or; ii) L-ara, to induce expression. Single plasmid strains were treated in the same way, except omitting Cm from the growth conditions.

β-galactosidase assays

Liquid assays for LacZ activity were performed using the substrate 4'-Methylumbelliferyl-β-D-glucuronide (MUG) as described before (43). Briefly, samples of culture (150 µl) were taken at each time point and frozen at –80°C until required. Ten µl aliquots of each sample culture were frozen at –80°C for 10 min and then thawed at room temperature. Next, 100-µl reaction buffer (PBS, 400 µg ml^{-1} lysozyme, 250 µg ml^{-1} MUG) was added and samples were immediately monitored in a Gemini XPS plate reader with the following parameters: excitation 360 nm, emission 450 nm, cut-off 435 nm, eight reads per well, and measured every 30 s for 30 min. RFU min^{-1} was calculated from a period of linear increase in fluorescence, normalized to the OD$_{600}$ of the sample.

11

Pulldown of ToxIN$_{Pa}$ and M1-23 from cell lysates

235

236 Using ΦM1 and ΦM1-O genomic DNA (gDNA), ΦM1-23 and M1-O-23 were amplified via

237 PCR using TRB111 and TRB135 as primers. The products were then digested using the relevant

238 restriction enzymes, ligated into pQE-80L and then used to transform ER2566. For the ToxIN$_{Pa}$

239 strains, pMJ4 (which contains ToxIN$_{Pa}$-FLAG) was used and a new plasmid was constructed to

240 make a ToxN$_{Pa}$-chitin binding domain (CBD) fusion. This was produced using pTA46 and

241 primers TRB37 and TRB38. The plasmid pTRB14 was then used to transform ER2566 which

242 had previously been transformed with pTRB18-KP14 that contains a ToxI$_{Pa}$ sequence.

243 Expression strains were grown in 2xYT media (per litre: 16 g tryptone, 10 g yeast extract,

244 5 g NaCl) at 37°C until an OD$_{600}$ of approximately 1. The cultures were then induced with the

245 appropriate supplement (0.5 mM IPTG for M1-23-6His and M1-O-23-6His) and then left to

246 grow overnight at 18°C. No inducers were added to the tagged ToxIN$_{Pa}$ containing strains as it is

247 constitutively expressed on pBR322.

248 Cells were harvested by centrifugation at 8,000 x g and the pellets were re-suspended in

249 10 ml lysis buffer (50 mM NaH$_2$PO$_4$.2H$_2$0, 500 mM NaCl, 10 mM imidazole, 10% glycerol, pH

250 8.0) per 500 ml of original culture volume. Cells were then lysed by four passes through a high-

251 pressure homogeniser (emulsiflex at up to 15,000 psi). Lysed cells were centrifuged at 8,000 x g

252 and the supernatants kept for further co-immunoprecipitation experiments.

253 In the experiments using M1-23-6His and M1-O-23-6His as bait, 1.5 ml Ni^{2+} resin

254 columns were used with ToxIN$_{Pa}$-FLAG. The columns were equilibrated using 3 column

255 volumes (CV) of lysis buffer before loading of the His-tagged protein lysates onto the resin.

256 Loaded resins were washed with 5 column volumes (CV) of wash buffer 1 (20 mM imidazole)

257 followed by 10 CV of wash buffer 2 (40 mM imidazole). The FLAG-tagged ToxIN$_{Pa}$ was then

258   loaded onto the appropriate columns via continuous flow for at least 3 h (often overnight) before

259   washing with 5 CV wash buffer 1 and 10 CV wash buffer 2.

260   Samples were eluted from the resin using elution buffer (250 mM imidazole) via 3 x 1 ml

261   fractions and analysed by western blot analysis using antibodies against His- (Novagen) and

262   FLAG- (Sigma) tags. Briefly, samples were run on 12.5 % Tris-tricine gels and transferred onto

263   Immobilon-P PVDF membranes (pore size: 0.45 µm; Millipore) at 250 mA for 90 min.

264   Membranes were then blocked with a 5% milk + PBST solution for 1 h before incubation with

265   anti-His and anti-FLAG antibodies at 1:10,000 for 2 h. After incubation, the membranes were

266   washed 3x 5 min in PBST and then incubated with the secondary anti-mouse antibody (Sigma) at

267   1:10,000 for 1 h before washing again 3x 5 min in PBST. The blots were then probed with

268   Immobilon-Western chemiluminescent HRP-substrate (Millipore) and developed.

269   For experiments where $ToxIN_{Pa}$ was used as the bait, the strain expressing $ToxIN_{Pa}$-CBD

270   was used with a 1 ml chitin resin. The protocol and buffers used were as described by the

271   manufacturer (NEB). Briefly, the $ToxIN_{Pa}$-CBD lysate was loaded onto the column and washed

272   with 40 ml of column buffer. The M1-23 or control pQE-80L lysates were then added onto their

273   respective columns. The columns were washed twice with 10 ml then 27 ml of column buffer

274   followed by a DTT flush, 5-7 ml for 10 min. Columns were then left to incubate overnight at

275   room temperature. After incubation, elution was carried out using 15 ml of column buffer.

276   Western blots were then performed on the samples as previously described.

277

278   **Measuring $ToxI_{Pa}$ levels after $ToxIN_{Pa}$ pulldowns with M1-23**

279    $ToxI_{Pa}$ levels were measured in the eluted fractions of the $ToxIN_{Pa}$-CBD, chitin resin column

280   experiments. Samples from cultures expressing either M1-23 or containing the pQE-80L vector

281   control were separated by electrophoresis at 80 volts, using a 1% w v^{-1} agarose gel made with

282   0.5x TAE. Additionally, samples were also measured by Nanodrop (Labtech, ND-1000).

283

284   **Co-immunoprecipitation of UvrA and M1-23**

285   UvrA-6His was constructed by amplification from the *E. coli* W3110 genome using primers

286   TRB337 and TRB338. PCR products were then digested with the appropriate restriction

287   enzymes and the digested product was purified, then ligated into pQE-80L to generate UvrA

288   with an N-terminal His-tag, pTRB301. This plasmid was then used to transform the *E. coli*

289   expression strain ER2566. Likewise, UvrA-FLAG was constructed in a similar way but using

290   primers TRB330 and TRB332 and ligated into pBAD33.

291   Expression and subsequent experiments were performed as described earlier using His-

292   tagged proteins as bait on Ni^{2+} resin. Expression of UvrA-FLAG was induced by addition of

293   0.02% arabinose.

294

295   **Construction of the *P. atrosepticum uvrA* mutant**

296   The *uvrA* mutant of Pba was constructed via allelic exchange. This was performed using the

297   plasmid pKNG-uvrA, which was derived from pKNG101. The plasmid was constructed by

298   firstly amplifying 500 bp regions up- and downstream of the *uvrA* gene in *P. atrosepticum*

299   SCRI1043. These two sequences were then ligated together with a kanamycin cassette inserted

300   in-between.

301   The suicide vector derivative, pKNG-uvrA, was used to transform *E. coli* β2163 and

302   grown overnight in the appropriate selective media. This acted as the donor strain and, along

14

303 with an overnight of the recipient strain, *P. atrosepticum* SCRI1043, was pelleted and

304 resuspended in LB. Both cultures were then mixed in the ratios of 2:1, 1:1 and 1:2 up to a final

305 volume of 100 µl. The resulting mixtures were then spotted on to DAPA-containing plates and

306 incubated at 25°C for 24 h. After mating, the patches were resuspended in 100 µl LB, serially

307 diluted and spread onto LBA plates containing tetracyline. These plates were incubated for 2 d at

308 25°C and colonies that appeared were picked and grown in LB overnight. The subsequent

309 overnight cultures were serially-diluted and 50 µl samples plated onto LBA plates containing

310 10% w v^{-1} sucrose. Colonies were also patched onto LBA plates containing kanamycin and the

311 gene deletion was confirmed using colony PCR and DNA sequencing. The strain was confirmed

312 phenotypically as UvrA-negative by demonstrating a hypersensitivity to UV light (Fig. S1).

313

314 **Genomic sequence accession number**

315 The genome of ΦM1 has been submitted to GenBank under the accession number JX290549.

316

317

318

319

320

321

322

15

323   **RESULTS**

324   **ΦM1 is a 'KMV-like' virus**

325   ΦM1 is a generalized transducing phage of *Pectobacterium atrosepticum* (Pba; previously

326   *Erwinia carotovora* subsp. *atroseptica*) (30). This Podovirus is aborted by the Type III TA

327   system, ToxIN from Pba, ToxIN$_{Pa}$ (22). ΦM1 generates spontaneous 'escape' mutants that are

328   resistant to Abi by ToxIN$_{Pa}$, at a rate of $\sim 10^{-5}$ (29). In order to improve our understanding of

329   ToxIN$_{Pa}$-phage interactions we sequenced ΦM1 wt and three previously isolated escape phages,

330   ΦM1-A, -B and -D (29).

331   Using BLAST searches (35), ΦM1 was classified as a member of the "KMV-like"

332   subgroup of the T7 supergroup of phages (44). T7-like phage linear genomes are typically

333   flanked by direct terminal repeats (DTRs) (45). However, the DTRs could not be defined by a

334   'primer walking' strategy along the ΦM1 genome, consistent with results from another "KMV-

335   like" phage, LIMEzero (46). The presence and approximate size of the DTRs, 293 bp, was

336   therefore confirmed through restriction digest analysis of the ΦM1 genome (Fig. S2). The final

337   ΦM1 wild type genome was 43,827 bp long with a GC content of 49.30%. In comparison, the

338   host Pba genome has a GC content of 50.97% (31). The two genomes therefore closely match

339   one another in GC content.

340   Global nucleotide alignments were performed to assess the relationship between the

341   "KMV-like" phages and ΦM1. When compared with ΦM1, phage VP93 (43,931 bp) (47), phage

342   LKA1 (41,593 bp) (44), phage LKD16 (43,200 bp) (44) and ΦKMV itself (42,519 bp) (45)

16

343 shared between 48.2% to 49.2% sequence identity. These values match well to those of other

344 "KMV-like" phages (46).

345 ΦM1 encodes 52 putative genes, named *phiM1-1* to *phiM1-52*. The gene products were

346 named M1-1 to M1-52 and they are encoded by 92.6% of the genome. Subsequent BLASTp

347 searches identified homologues for 32 of the ORFs, from other "KMV-like" phages (Table S1).

348 In most cases it was therefore possible to assign putative functions and categorize ORFs as

349 encoding either metabolism, structural or host lysis genes (Fig. 1A). ΦM1 also encodes a single

350 tRNA^{Ile}, between *phiM1-38* and *phiM1-39*.

351

352 **ΦM1 escape mutations had specific base substitutions**

353 The genome sequences of the three escape phages, M1-A, -B and -D, were compared with that of

354 the wt. All three escape phages had single point mutations localized to a 124 bp stretch (Fig. 1B),

355 across *phiM1-22* and *phiM1-23*, which we refer to as the "escape locus". To ascertain whether

356 these point substitutions were individual changes, further escape phages were isolated using

357 independent lysates to avoid the possibility of sibling mutants. The new escape phage mutants

358 were isolated following selection on Pba pTA46 (ToxIN$_{Pa}$) (22, 29). The escape locus of each

359 phage was sequenced following amplification of the region from the purified genomic DNA. We

360 observed that all 10 escape phages had unique mutations distributed across 246 bp of the escape

361 locus (Fig. 1B). Nine of these mutations were base substitutions while one was a single base

362 deletion (Table 4).

17

Infection with ΦM1 affects the $ToxI_{Pa}$:$ToxN_{Pa}$ ratio

364   Though it has been shown that $ToxN_{Pa}$ levels do not alter during an ΦM1 phage infection (29), it

365   was not known how the $ToxI_{Pa}$ levels were affected. The identification of the escape phages

366   provided an opportunity to address this question. To investigate alterations to the $ToxI_{Pa}$:$ToxN_{Pa}$

367   ratio, we monitored the levels of $ToxI_{Pa}$ and $ToxN_{Pa}$-FLAG during the infections by ΦM1 and

368   the escape phage, ΦM1-O, within Pba carrying a $ToxIN_{Pa}$-FLAG plasmid (pMJ4). Total protein

369   and RNA samples were taken at different times after infection and subjected to Western Blot and

370   S1-nuclease assay, respectively. While $ToxN_{Pa}$ levels stayed constant throughout infection (Fig.

371   2A, lower panel), $ToxI_{Pa}$ levels dropped dramatically after 30 minutes compared to an uninfected

372   control (Fig. 2A). Interestingly, $ToxI_{Pa}$ levels increased back to original levels at 60 minutes. In

373   comparison to the infection with ΦM1 wt, $ToxI_{Pa}$ levels did not change significantly at 30

374   minutes during infection with the escape phage ΦM1-O (Fig. 2B). The $ToxI_{Pa}$ level did decrease

375   with the ΦM1-O infection, but only at 40 minutes (Fig. 2B). The $ToxI_{Pa}$ levels were not then

376   restored, as in the case of ΦM1 wt (Fig. 2B). ΦM1 appears to activate $ToxN_{Pa}$, and thereby

377   initiate Abi, by causing a decrease in the cellular $ToxI_{Pa}$ levels, either through direct or indirect

378   means. In the case of ΦM1-O, this activation is prevented due to the mutation in M1-23. This

379   would allow the phage to propagate, which may then account for the delayed decrease and lack

380   of restoration in $ToxI_{Pa}$ levels.

381

382

383

18

Identification and characterization of the ΦM1 escape product

384

385   The majority of escape mutations occurred within *phiM1-23*. On first analysis, two mutations,

386   those from ΦM1-B and ΦM1-X, occurred at the 3′ end of *phiM1-22*. Another mutation, from

387   ΦM1-C, mapped further upstream, again within *phiM1-22*. This gene, *phiM1-22*, encodes a

388   homologue of a putative DNA exonuclease from phage LKA1 (Table S1) (44). Unfortunately,

389   there were no database hits for *phiM1-23* and *phiM1-24*, using either the nucleotide or encoded

390   protein sequences.

391   Specific regions of this escape locus were amplified from ΦM1 phages, then cloned into

392   pBAD30 (48) to make inducible constructs (Fig. 3A and 3B). The cloning began with constructs

393   1-6, using DNA from ΦM1 wt and ΦM1-B (Fig. 3B). Constructs 1 and 2 could not be obtained

394   with ΦM1 wt DNA presumably through toxicity of the resulting wt constructs in *E. coli* DH5α,

395   though could be made using ΦM1-B escape phage DNA. Constructs 3, 4, 5 and 6 could be made

396   using both sources of DNA. Due to the regions covered by these constructs we could determine

397   that within this locus the genes of interest were *phiM1-22* and *phiM1-23*, and that *phiM1-24* did

398   not contribute to toxicity. As pBAD30 is tightly repressed by glucose in *E. coli* DH5α, this also

399   implied that toxicity from this region of DNA might be occurring via an internal promoter.

400   Upon first analysis, the putative ATG start of *phiM1-23* was at 15,304 bp. Taking into

401   account the STOP codons of each frame (green vertical lines, Fig. 1B), the putative ATG start

402   codon of *phiM1-23* could theoretically have been upstream of this initial annotation. There were

403   three possible ATG sites upstream of the putative start codon for *phiM1-23*. The mutation of

404   ΦM1-C specifically altered the middle of these start codons from M to T (Table 4). This start

405   codon also had a ribosome binding site closer to consensus than those of the other potential start

406   codons, making it the most obvious candidate. If this were the case, the escape mutations would

407   span *phiM1-23* specifically. Constructs 7-9 were designed and made, in order to test whether

408   *phiM1-23* alone could generate a toxic phenotype.

409   We performed experiments to assess the toxicity of the escape locus constructs and to

410   determine whether toxicity was related to the presence of ToxIN$_{Pa}$. Pba was transformed with

411   inducible derivatives of the escape locus in combination with either pBluescript-based

412   (Fermentas) ToxIN$_{Pa}$ or negative control ToxIN$_{Pa}$-frameshift (FS) vectors (pTRB125 and

413   pTRB126, respectively). Serial dilutions of these dual-vector strains of Pba were then incubated

414   with and without induction, overnight, to determine the viable count (Fig. 3C). This clearly

415   showed that the product of construct 7, covering *phiM1-23* specifically, was toxic. There was no

416   toxicity in the case of ΦM1-B, the mutation in which causes a premature STOP codon in *phiM1-*

417   *23*. Toxicity was also independent of the presence of ToxIN$_{Pa}$. These results strongly suggested

418   that *phiM1-23* produces a small, toxic protein, responsible either directly or indirectly, for

419   activation of Abi against ΦM1.

420   New versions of construct 7 (Fig. 3D) were then generated, adding a C-terminal FLAG

421   tag to the M1-23 product, using both ΦM1 wt and escape sequences. Various constructs were

422   then tested for toxicity in the cognate host, Pba (Fig. 3D). All the escape constructs tested

423   showed reduced toxicity (Fig. 3D). It was therefore possible to attempt over-expression and

424   purification of M1-23, using an *E. coli* expression strain, ER2566. After expression trials using

425   constructs made from ΦM1 wt, -O, -W and -Y phage DNA, the M1-O-23FLAG product was

426   chosen for further study. Sufficient M1-O-23FLAG protein was purified to allow mass

427   spectrometry to confirm both the identity of the protein, and specifically the presence of the

428   expected Q to P mutation. Furthermore, the protein sample was subjected to N-terminal

429   sequencing, generating a sequence of TKM. This implied that *phiM1-23* started at the ATG

430   specifically mutated by ΦM1-C, as described earlier, and that the initial methionine is cleaved

431   post-translationally. The annotation of the ΦM1 wt genome was then altered to accommodate

432   *phiM1-23* beginning at this confirmed start codon. In summary, this result shows that all the

433   escape mutations map to a single gene, *phiM1-23*, which generates a 9.8 kDa protein. These

434   mutations reduce toxicity of the protein product, and allow viral escape from ToxIN$_{Pa}$-induced

435   Abi.

436   It had not been possible to clone constructs 1 and 2 (Fig. 3B) using the ΦM1 wt

437   sequence, despite the pBAD30 vector system being repressed in the presence of glucose. This

438   suggested that a promoter internal to those cloned regions might be inducing transcription of

439   *phiM1-23*. A range of pRW50-based (49), *lacZ* transcriptional fusion constructs was generated to

440   investigate the possible presence of a promoter (Fig. S3A). In this case, it was possible to clone

441   the equivalent of construct 2 using ΦM1 wt DNA (Fig. 3B), perhaps due to pRW50 having a low

442   copy number, so the level of toxicity was sufficiently low. Plasmid pTA104 (22), containing the

443   promoter for ToxIN$_{Pa}$, was used as a positive control. All the test constructs except pTRB162,

444   which was an extremely truncated clone, generated LacZ activity (Fig. S3B). This confirmed the

445   presence of a weak *phiM1-23* promoter within *phiM1-22*.

446

447   **Extensive analysis of ΦM1 escape mutants map all mutations to *phiM1-23***

448   The initial 10 escape mutants of ΦM1 all had unique mutations in M1-23, so it was likely that

449   there were other possible mutations not yet observed. Identifying these other mutations could

450   reveal important residues involved in the functionality of M1-23. Consequently, a larger library

451   of escape mutants was isolated and characterized in the same way as the initial escapes. A total

452   of 51 new, independent escape phages were isolated and their *phiM1-23* sequences were

453   characterized. All escapes were shown to have a mutation in this region and several new unique

454   escapes were isolated (Table S2). With the addition of these new escapes the number of different

455   mutations increased to 20. Interestingly, mutations in all three of the bases of the putative start

456   codon were isolated, consistent with this being the correctly annotated start site. Other interesting

457   mutations were those causing N-terminally located truncations of M1-23. In particular, ΦM1-

458   E11 produced only a hypothetical dipeptide or indeed just a single amino acid if the intial

459   starting methionine were removed. Although most mutations in M1-23 were missense alleles

460   generating single amino acid residue changes, the ability to isolate derivatives with major

461   truncations showed that the M1-23 protein must be non-essential for a productive ΦM1 lytic

462   cycle. Other notable mutations were ΦM1-E48 and 49 (both generating the same outcome),

463   which modify the stop codon and lead to a 10 amino acid C-terminal extension. It is puzzling

464   why the 10-mer extension might impact function, because the addition of the octameric FLAG

465   tag to the C-terminus of M1-23 did not disrupt protein toxicity. Perhaps the extension might

466   harbour a sequence that could act as an auto-inhibitor or disrupt protein structure.

467

468   **M1-23 interacts with UvrA but abortive infection can still take place in UvrA-**

469   **deficient *P. atrosepticum***

470   To assess whether there is a direct interaction of M1-23 with the ToxIN$_{Pa}$ complex, His-tagged

471   forms of both M1-23 and M1-O-23 were cloned, allowing over-expression and purification of

472   these proteins. Co-immunoprecipitation reactions were carried out but the results showed no

473   evidence for interactions between M1-23 and the ToxIN$_{Pa}$ complex, and that M1-23 had no

474   impact on the ToxI RNA (data not shown).

22

475   During the process of purifying M1-23-6His it was noted that an additional high

476   molecular weight band appeared in the eluted sample that was not present in control samples,

477   which then co-purified with M1-23 following ion exchange FPLC (data not shown). Mass

478   spectrometric analysis identified the host nucleotide excision repair protein, UvrA. Reciprocal

479   co-immunoprecipitation assays were performed using purified protein samples to confirm this

480   interaction (Fig. 4). M1-23 protein retained UvrA while M1-O-23 did not, and similarly, only

481   M1-23 was retained by immobilized UvrA (Fig. 4). This strongly suggests that M1-23 is a viral

482   product that is able to bind host UvrA.

483   To assess potential effects of UvrA in abortive infection, a *uvrA* mutant was constructed

484   in *P. atrosepticum*, confirmed by sequencing and then by hypersensitivity to UV light (Fig. S1).

485   This strain was tested for its ability to abort ΦM1 via the ToxIN$_{Pa}$ system. Surprisingly, ΦM1

486   was still aborted in the *uvrA* mutant and to the same extent as in the wild type Pba strain (EOP of

487   ΦM1 on *uvrA* mutant with ToxIN$_{Pa}$ is 1.1×10^{-5}). Escapes of ΦM1 were isolated from the *uvrA*

488   mutant and their DNA was sequenced. Interestingly, all escapes isolated on the *uvrA* mutant,

489   ΦM1-U1, U2 and ΦM1-U4 to U10 (which were independently isolated), carried mutations in the

490   M1-23 sequence (Table S2). The results suggest that although M1-23 clearly has a specific

491   interaction with UvrA, it appears that the escape route is either subtle or occurs indirectly.

492

493   **The ΦM1 escape mechanism works in another Type III TA and Abi system**

494   Two further families of Type III TA systems were recently identified, CptIN and TenpIN (23).

495   TenpIN$_{Pl}$, from the chromosome of *Photorhabdus luminescens* TT01, was able to act as an Abi

496   system against coliphages when cloned on a multicopy plasmid and tested in an *E. coli*

497 background (23). By transforming *P. atrosepticum* SCRI1043 with the TenpIN$_{Pl}$ expression

498 plasmid, pFR2 (23), we were able to test three *Pectobacterium* phages against the Abi activity of

499 TenpIN$_{Pl}$ (Table 5). While ΦS61 (29) and ΦTE (27) were dramatically affected by ToxIN$_{Pa}$,

500 neither were inhibited by TenpIN$_{Pl}$ (Table 5). This indicates a degree of selectivity between the

501 two Abi systems. ΦM1, however, was aborted by both systems, though to different degrees,

502 which also underlines the selectivity under which ToxIN$_{Pa}$ and TenpIN$_{Pl}$ appear to operate. As

503 with ToxIN$_{Pa}$, it was possible to select for phages of ΦM1 that escaped Abi by TenpIN$_{Pl}$. One of

504 these escape phages, ΦM1-PL2, was isolated and sequenced. This escape phage had a single

505 base substitution, T15410C, the same mutation as ΦM1-D. To test this in reverse, escape phage

506 ΦM1-O, selected with ToxIN$_{Pa}$, was tested against TenpIN$_{Pl}$ (Table 5). ΦM1-O was also

507 resistant to TenpIN$_{Pl}$. These results imply that, in the case of ΦM1, both systems operate in a

508 similar fashion with a single protein, M1-23, being a key mediator.

509

510

511

512

513

514

515

516

517

24

DISCUSSION

519 The pectobacterial phage ΦM1 was shown previously to be sensitive to the ToxIN$_{Pa}$ system and

520 capable of producing spontaneous escape mutants (29). Here we found that the ΦM1 phage is

521 also sensitive to TenpIN$_{Pl}$ when reconstructed in *P. atrosepticum* and is correspondingly able to

522 evolve escape mutants. This is the first time we have been able to identify a phage able to escape

523 the TenpIN$_{Pl}$ system and so further study may provide information about its activation.

524 Interestingly, the ΦM1 phage is insensitive to two other Type III systems tested, ToxIN$_{Bt}$ from

525 *Bacillus thuringiensis* and the CptIN$_{Er}$ system from *Eubacterium rectale* (data not shown) and no

526 Abi activity has so far been observed in these two systems (23, 50). In contrast, the *P.*

527 *atrosepticum* phage ΦTE is aborted by ToxIN$_{Pa}$ and able to escape the system by RNA-based

528 molecular mimicry of the antitoxin (27) but is not aborted by the TenpIN$_{Pl}$ system (Table 5).

529   Characterization of the ΦM1 phage in this study has shown that all escapes selected on

530 ToxIN$_{Pa}$ or TenpIN$_{Pl}$ have mutations in a gene encoding M1-23. Alteration of single amino acids,

531 extreme truncations due to very 5′ stop codons, or even stop codon mutations leading to short C-

532 terminal extensions of M1-23 cause insensitivity to both ToxIN$_{Pa}$ and TenpIN$_{Pl}$. Escapes selected

533 on one system are also insensitive to the other system, suggesting that there is a common

534 pathway for the ΦM1 phage in the activation of these two systems. The role of M1-23 is

535 unknown, but it was shown to be non-essential and as it is located between a predicted

536 exonuclease *phiM1-22* and a predicted endonuclease gene *phiM1-25*, it could have a role in the

537 regulation of nucleases or indeed may be able to act as a nuclease itself. In a previous study it

538 was shown that ToxN$_{Pa}$ levels do not change during infection of the ΦM1 phage (29). In this

539 study we found that the ToxI$_{Pa}$ levels decrease 30 minutes post-infection. In contrast, during the

540 infection by the ΦM1 escape phage, ΦM1-O, ToxI$_{Pa}$ levels only slightly decreased after 40

541 minutes and were not restored. It appears that wild type ΦM1 activates ToxN$_{Pa}$ by decreasing the

542 levels of ToxI$_{Pa}$ and therefore initiating Abi. For ΦM1-O, the mutation in M1-23 prevents this

543 early activation and thereby provides a window of opportunity for the phage to replicate.

544   To investigate the mechanism of M1-23 action, a large number of ΦM1 escape phages

545 were isolated and their *phiM1-23* regions were sequenced. The results showed a number of

546 escape mutations near the 5′ end of the gene, resulting in extremely truncated versions of the

547 protein. This confirms that M1-23 is a non-essential viral protein. However, the majority of

548 mutations found were towards the 3′ region of the gene and were mostly missense mutations

549 resulting in single amino acid changes, implying that the C-terminal domain of the protein is

550 important for Abi functionality. To further characterize M1-23, it was overexpressed and purified

551 but, due to high toxicity, only a small amount of protein could be produced. Using the limited

552 amount of protein available, interaction studies were performed to see if M1-23 interacted with

553 ToxIN$_{Pa}$. During purification of M1-23, a high molecular weight protein always co-purified.

554 Mass spectrometry of this protein confirmed that it was the DNA repair protein UvrA. It was

555 shown through co-immunoprecipitation experiments that while M1-23 could interact with UvrA,

556 the escape version of the protein M1-O-23 could not.

557   UvrA forms part of the SOS response in bacteria - a DNA damage response pathway (51)

558 that has previously been shown to be involved in TA activation. The Type I TA system TisB-

559 IstR is under direct SOS response control, as *tisAB* which encodes the TisB toxin contains a

560 LexA operator region that is inhibited by LexA (52). As well as the SOS response, the stringent

561 response has also been shown to play a role in the activation of TA systems. Both Type I and

562 Type II TA systems have been shown to be regulated by (p)ppGpp, the central regulator of the

563   stringent response (53, 54). However, ΦM1 and ΦTE were tested in a (p)ppGpp negative double

564   mutant (*relA, spoT*) and were still aborted in that background (data not shown).

565   During the course of this study, two new pectobacterial phage genomes were sequenced.

566   These were *P. atrosepticum* phage Peat1 (55), (GenBank accession KR604693) and *P.*

567   *carotovorum* phage PPWS1 (56), (DDBJ accession number LC063634). Both of these were

568   podoviruses that shared high sequence identity to ΦM1. Peat1 (45,6533 bp) shared 77.7%

569   sequence identity and PPWS1 (44,539 bp) shared 59.7% sequence identity. Furthermore,

570   analysis of both genomes revealed that both phages encoded M1-23 homologs with the Peat1

571   homolog only differing by a single amino acid. Therefore, it is highly likely that both phages

572   would be aborted by both the $ToxIN_{Pa}$ and $TenpIN_{Pl}$ systems and evolve escapes in the same

573   way. If this was the case, it would show a common route through which phages of different

574   bacteria are able to escape the same system.

575   Both $ToxIN_{Pa}$ and $TenpIN_{Pl}$ are very powerful anti-phage abortive infection systems that

576   belong to two different families of Type III TA systems and are effective against a wide variety

577   of phages. While many phages show differing sensitivity to the two systems, this study has

578   shown that in ΦM1 there is a common pathway through which these two families of Type III TA

579   systems can be activated. This pathway involves a small toxic protein, M1-23, of unknown

580   metabolic function that does not directly interact with the $ToxIN_{Pa}$ complex, but interacts directly

581   with UvrA. ΦM1 infection causes a diminution in $ToxI_{Pa}$ levels presumably leading to the

582   destabilization of the $ToxIN_{Pa}$ complex and consequent liberation of $ToxN_{Pa}$ to induce cell death

583   and concomitant abortive infection of the viral parasite.

584

592 **REFERENCES**

593 1. **Wommack KE, Colwell RR.** 2000. Virioplankton: viruses in aquatic ecosystems. Microbiol Mol

594   Biol Rev **64:**69-114.

595 2. **Chibani-Chennoufi S, Bruttin A, Dillmann ML, Brüssow H.** 2004. Phage-host interaction: an

596   ecological perspective. J Bacteriol **186:**3677-3686.

597 3. **Dy RL, Richter C, Salmond GP, Fineran PC.** 2014. Remarkable Mechanisms in Microbes to Resist

598   Phage Infections. Annu Rev Virol **1:**307-331.

599 4. **Stern A, Sorek R.** 2011. The phage-host arms race: shaping the evolution of microbes. Bioessays

600   **33:**43-51.

601 5. **Loenen WA, Dryden DT, Raleigh EA, Wilson GG, Murray NE.** 2014. Highlights of the DNA

602   cutters: a short history of the restriction enzymes. Nucleic Acids Res **42:**3-19.

603 6. **Doudna JA, Charpentier E.** 2014. Genome editing. The new frontier of genome engineering with

604   CRISPR-Cas9. Science **346:**1258096.

605 7. **Chopin MC, Chopin A, Bidnenko E.** 2005. Phage abortive infection in lactococci: variations on a

606   theme. Curr Opin Microbiol **8:**473-479.

607 8. **Cavanagh D, Fitzgerald GF, McAuliffe O.** 2015. From field to fermentation: the origins of

608   *Lactococcus lactis* and its domestication to the dairy environment. Food Microbiol **47:**45-61.

609 9. **Parma DH, Snyder M, Sobolevski S, Nawroz M, Brody E, Gold L.** 1992. The Rex system of

610   bacteriophage lambda: tolerance and altruistic cell death. Genes Dev **6:**497-510.

611 10. **Georgiou T, Yu YN, Ekunwe S, Buttner MJ, Zuurmond A, Kraal B, Kleanthous C, Snyder L.** 1998.

612   Specific peptide-activated proteolytic cleavage of Escherichia coli elongation factor Tu. Proc Natl

613   Acad Sci U S A **95:**2891-2895.

614 11. **Penner M, Morad I, Snyder L, Kaufmann G.** 1995. Phage T4-coded Stp: double-edged effector of

615   coupled DNA and tRNA-restriction systems. J Mol Biol **249:**857-868.

29

616   12.   **Yamaguchi Y, Park JH, Inouye M.** 2011. Toxin-antitoxin systems in bacteria and archaea. Annu

617   Rev Genet **45:**61-79.

618   13.   **Gerdes K, Rasmussen PB, Molin S.** 1986. Unique type of plasmid maintenance function:

619   postsegregational killing of plasmid-free cells. Proc Natl Acad Sci U S A **83:**3116-3120.

620   14.   **Ramage HR, Connolly LE, Cox JS.** 2009. Comprehensive functional analysis of *Mycobacterium*

621   *tuberculosis* toxin-antitoxin systems: implications for pathogenesis, stress responses, and

622   evolution. PLoS Genet **5:**e1000767.

623   15.   **Christensen SK, Gerdes K.** 2003. RelE toxins from bacteria and Archaea cleave mRNAs on

624   translating ribosomes, which are rescued by tmRNA. Mol Microbiol **48:**1389-1400.

625   16.   **Lehnherr H, Maguin E, Jafri S, Yarmolinsky MB.** 1993. Plasmid addiction genes of bacteriophage

626   P1: doc, which causes cell death on curing of prophage, and phd, which prevents host death

627   when prophage is retained. J Mol Biol **233:**414-428.

628   17.   **Page R, Peti W.** 2016. Toxin-antitoxin systems in bacterial growth arrest and persistence. Nat

629   Chem Biol **12:**208-214.

630   18.   **Brantl S, Jahn N.** 2015. sRNAs in bacterial type I and type III toxin-antitoxin systems. FEMS

631   Microbiol Rev **39:**413-427.

632   19.   **Pecota DC, Wood TK.** 1996. Exclusion of T4 phage by the hok/sok killer locus from plasmid R1. J

633   Bacteriol **178:**2044-2050.

634   20.   **Hazan R, Engelberg-Kulka H.** 2004. *Escherichia coli* mazEF-mediated cell death as a defense

635   mechanism that inhibits the spread of phage P1. Mol Genet Genomics **272:**227-234.

636   21.   **Otsuka Y, Yonesaki T.** 2012. Dmd of bacteriophage T4 functions as an antitoxin against

637   *Escherichia coli* LsoA and RnlA toxins. Mol Microbiol **83:**669-681.

30

638   22.   **Fineran PC, Blower TR, Foulds IJ, Humphreys DP, Lilley KS, Salmond GP.** 2009. The phage

639   abortive infection system, ToxIN, functions as a protein-RNA toxin-antitoxin pair. Proc Natl Acad

640   Sci U S A **106:**894-899.

641   23.   **Blower TR, Short FL, Rao F, Mizuguchi K, Pei XY, Fineran PC, Luisi BF, Salmond GP.** 2012.

642   Identification and classification of bacterial Type III toxin-antitoxin systems encoded in

643   chromosomal and plasmid genomes. Nucleic Acids Res **40:**6158-6173.

644   24.   **Samson JE, Spinelli S, Cambillau C, Moineau S.** 2013. Structure and activity of AbiQ, a

645   lactococcal endoribonuclease belonging to the type III toxin-antitoxin system. Mol Microbiol

646   **87:**756-768.

647   25.   **Dy RL, Przybilski R, Semeijn K, Salmond GP, Fineran PC.** 2014. A widespread bacteriophage

648   abortive infection system functions through a Type IV toxin-antitoxin mechanism. Nucleic Acids

649   Res **42:**4590-4605.

650   26.   **Sberro H, Leavitt A, Kiro R, Koh E, Peleg Y, Qimron U, Sorek R.** 2013. Discovery of functional

651   toxin/antitoxin systems in bacteria by shotgun cloning. Mol Cell **50:**136-148.

652   27.   **Blower TR, Evans TJ, Przybilski R, Fineran PC, Salmond GP.** 2012. Viral evasion of a bacterial

653   suicide system by RNA-based molecular mimicry enables infectious altruism. PLoS Genet

654   **8:**e1003023.

655   28.   **Samson JE, Bélanger M, Moineau S.** 2013. Effect of the abortive infection mechanism and type

656   III toxin/antitoxin system AbiQ on the lytic cycle of *Lactococcus lactis* phages. J Bacteriol

657   **195:**3947-3956.

658   29.   **Blower TR, Fineran PC, Johnson MJ, Toth IK, Humphreys DP, Salmond GP.** 2009. Mutagenesis

659   and functional characterization of the RNA and protein components of the toxIN abortive

660   infection and toxin-antitoxin locus of *Erwinia*. J Bacteriol **191:**6029-6039.

661   30.   **Toth IK, Mulholland V, Cooper V, Bentley S, Shih Y, -L., Perombelon MCM, Salmond GPC.** 1997.

662   Generalized transduction in the potato blackleg pathogen *Erwinia carotovora* subsp. *atrospetica*

663   by bacteriophage phi M1. Microbiology **143:**2433-2438.

664   31.   **Bell KS, Sebaihia M, Pritchard L, Holden MT, Hyman LJ, Holeva MC, Thomson NR, Bentley SD,**

665   **Churcher LJ, Mungall K, Atkin R, Bason N, Brooks K, Chillingworth T, Clark K, Doggett J, Fraser**

666   **A, Hance Z, Hauser H, Jagels K, Moule S, Norbertczak H, Ormond D, Price C, Quail MA, Sanders**

667   **M, Walker D, Whitehead S, Salmond GP, Birch PR, Parkhill J, Toth IK.** 2004. Genome sequence

668   of the enterobacterial phytopathogen *Erwinia carotovora* subsp. *atroseptica* and

669   characterization of virulence factors. Proc Natl Acad Sci U S A **101:**11105-11110.

670   32.   **Petty NK, Foulds IJ, Pradel E, Ewbank JJ, Salmond GP.** 2006. A generalized transducing phage

671   (phiIF3) for the genomically sequenced *Serratia marcescens* strain Db11: a tool for functional

672   genomics of an opportunistic human pathogen. Microbiology **152:**1701-1708.

673   33.   **Lukashin AV, Borodovsky M.** 1998. GeneMark.hmm: new solutions for gene finding. Nucleic

674   Acids Res **26:**1107-1115.

675   34.   **Delcher AL, Harmon D, Kasif S, White O, Salzberg SL.** 1999. Improved microbial gene

676   identification with GLIMMER. Nucleic Acids Res **27:**4636-4641.

677   35.   **Altschul SF, Gish W, Miller W, Myers EW, Lipman DJ.** 1990. Basic local alignment search tool. J

678   Mol Biol **215:**403-410.

679   36.   **Suzek BE, Ermolaeva MD, Schreiber M, Salzberg SL.** 2001. A probabilistic method for identifying

680   start codons in bacterial genomes. Bioinformatics **17:**1123-1130.

681   37.   **Lowe TM, Eddy SR.** 1997. tRNAscan-SE: a program for improved detection of transfer RNA genes

682   in genomic sequence. Nucleic Acids Res **25:**955-964.

683   38.   **Reese MG.** 2001. Application of a time-delay neural network to promoter annotation in the

684   Drosophila melanogaster genome. Comput Chem **26:**51-56.

685   39.   **Rutherford K, Parkhill J, Crook J, Horsnell T, Rice P, Rajandream MA, Barrell B.** 2000. Artemis:

686   sequence visualization and annotation. Bioinformatics **16:**944-945.

687   40.   **Fineran PC, Everson L, Slater H, Salmond GP.** 2005. A GntR family transcriptional regulator

688   (PigT) controls gluconate-mediated repression and defines a new, independent pathway for

689   regulation of the tripyrrole antibiotic, prodigiosin, in *Serratia*. Microbiology **151:**3833-3845.

690   41.   **McNeil MB, Clulow JS, Wilf NM, Salmond GP, Fineran PC.** 2012. SdhE is a conserved protein

691   required for flavinylation of succinate dehydrogenase in bacteria. J Biol Chem **287:**18418-18428.

692   42.   **Przybilski R, Richter C, Gristwood T, Clulow JS, Vercoe RB, Fineran PC.** 2011. Csy4 is responsible

693   for CRISPR RNA processing in *Pectobacterium atrosepticum*. RNA Biol **8:**517-528.

694   43.   **Ramsay JP, Williamson NR, Spring DR, Salmond GP.** 2011. A quorum-sensing molecule acts as a

695   morphogen controlling gas vesicle organelle biogenesis and adaptive flotation in an

696   enterobacterium. Proc Natl Acad Sci U S A **108:**14932-14937.

697   44.   **Ceyssens PJ, Lavigne R, Mattheus W, Chibeu A, Hertveldt K, Mast J, Robben J, Volckaert G.**

698   2006. Genomic analysis of *Pseudomonas aeruginosa* phages LKD16 and LKA1: establishment of

699   the phiKMV subgroup within the T7 supergroup. J Bacteriol **188:**6924-6931.

700   45.   **Lavigne R, Burkal'tseva MV, Robben J, Sykilinda NN, Kurochkina LP, Grymonprez B, Jonckx B,**

701   **Krylov VN, Mesyanzhinov VV, Volckaert G.** 2003. The genome of bacteriophage phiKMV, a T7-

702   like virus infecting *Pseudomonas aeruginosa*. Virology **312:**49-59.

703   46.   **Adriaenssens EM, Van Vaerenbergh J, Vandenheuvel D, Dunon V, Ceyssens PJ, De Proft M,**

704   **Kropinski AM, Noben JP, Maes M, Lavigne R.** 2012. T4-related bacteriophage LIMEstone

705   isolates for the control of soft rot on potato caused by '*Dickeya solani*'. PLoS One **7:**e33227.

706   47.   **Bastías R, Higuera G, Sierralta W, Espejo RT.** 2010. A new group of cosmopolitan

707   bacteriophages induce a carrier state in the pandemic strain of *Vibrio parahaemolyticus*. Environ

708   Microbiol **12:**990-1000.

33

709   48.   **Guzman LM, Belin D, Carson MJ, Beckwith J.** 1995. Tight regulation, modulation, and high-level

710   expression by vectors containing the arabinose PBAD promoter. J Bacteriol **177:**4121-4130.

711   49.   **Lodge J, Fear J, Busby S, Gunasekaran P, Kamini NR.** 1992. Broad host range plasmids carrying

712   the *Escherichia coli* lactose and galactose operons. FEMS Microbiol Lett **74:**271-276.

713   50.   **Short FL, Pei XY, Blower TR, Ong SL, Fineran PC, Luisi BF, Salmond GP.** 2013. Selectivity and

714   self-assembly in the control of a bacterial toxin by an antitoxic noncoding RNA pseudoknot. Proc

715   Natl Acad Sci U S A **110:**E241-249.

716   51.   **Little JW, Mount DW.** 1982. The SOS regulatory system of *Escherichia coli*. Cell **29:**11-22.

717   52.   **Wagner EG, Unoson C.** 2012. The toxin-antitoxin system tisB-istR1: Expression, regulation, and

718   biological role in persister phenotypes. RNA Biol **9:**1513-1519.

719   53.   **Maisonneuve E, Castro-Camargo M, Gerdes K.** 2013. (p)ppGpp controls bacterial persistence by

720   stochastic induction of toxin-antitoxin activity. Cell **154:**1140-1150.

721   54.   **Verstraeten N, Knapen WJ, Kint CI, Liebens V, Van den Bergh B, Dewachter L, Michiels JE, Fu Q,**

722   **David CC, Fierro AC, Marchal K, Beirlant J, Versées W, Hofkens J, Jansen M, Fauvart M,**

723   **Michiels J.** 2015. Obg and Membrane Depolarization Are Part of a Microbial Bet-Hedging

724   Strategy that Leads to Antibiotic Tolerance. Mol Cell **59:**9-21.

725   55.   **Kalischuk M, Hachey J, Kawchuk L.** 2015. Complete Genome Sequence of Phytopathogenic

726   *Pectobacterium atrosepticum* Bacteriophage Peat1. Genome Announc **3**.

727   56.   **Hirata H, Kashihara M, Horiike T, Suzuki T, Dohra H, Netsu O, Tsuyumu S.** 2016. Genome

728   Sequence of *Pectobacterium carotovorum* Phage PPWS1, Isolated from Japanese Horseradish

729   [Eutrema japonicum (Miq.) Koidz] Showing Soft-Rot Symptoms. Genome Announc **4**.

730   57.   **Demarre G, Guérout AM, Matsumoto-Mashimo C, Rowe-Magnus DA, Marlière P, Mazel D.**

731   2005. A new family of mobilizable suicide plasmids based on broad host range R388 plasmid

34

732   (IncW) and RP4 plasmid (IncPalpha) conjugative machineries and their cognate *Escherichia coli*

733   host strains. Res Microbiol **156:**245-255.

734   58.   **Bachmann BJ.** 1972. Pedigrees of some mutant strains of *Escherichia coli* K-12. Bacteriol Rev

735   **36:**525-557.

736   59.   **Chang AC, Cohen SN.** 1978. Construction and characterization of amplifiable multicopy DNA

737   cloning vehicles derived from the P15A cryptic miniplasmid. J Bacteriol **134:**1141-1156.

738   60.   **Poulter S.** 2011. The LuxR-family quorum sensing transcriptional regulator CarR in *Erwinia* and

739   *Serratia*. PhD. University of Cambridge.

740

741

742 **Figure legends**

743

744 FIG 1 Genomic map of ΦM1 wild type and its escape locus. (A) All the fifty-two annotated

745 ORFs are coded on the forward reading strand, in a linear progression from metabolic genes, to

746 structural genes and finally host cell lysis genes. Each forward reading frame is labelled; F1, F2

747 or F3. ORFs are shown to scale as shaded boxes numbered with the gene number, coloured

748 according to predicted role. The single tRNA^{Ile} gene is positioned on the scale, shown in purple.

749 Where it has been possible to identify a protein by homology searches, that ORF is labelled. The

750 scale is in base-pairs. The figure was drawn to scale using Adobe Illustrator. (B) Schematic of

751 the escape locus of ΦM1. All escape phage mutations are within *phiM1-23*. Each forward

752 reading frame is labelled; F1, F2 or F3. Each ORF is shown to scale as a box, numbered with the

753 gene number. Each STOP codon is represented as a green vertical line. The positions of the ΦM1

754 escape phage mutations are shown by red vertical lines, labelled with the parent phage. The scale

755 is in base pairs.

756

757 FIG 2 ToxI$_{Pa}$ levels are affected during phage infection. (A) S1-nuclease assay targeting the full

758 5.5 repeat ToxI$_{Pa}$ sequence was used to monitor ToxI$_{Pa}$ levels during ΦM1 infection. Assays

759 were performed on 10 μg total RNA prepared from Pba ToxIN$_{Pa}$ (pMJ4) at different times

760 following ΦM1 infection. Numbers indicate the time (min) after infection with phage (+ ΦM1)

761 and the negative control without phage (- ΦM1). Hybridization to total RNA from Pba

762 expressing ToxIN$_{Pa}$ (pTA46) and DH5α served as positive and negative controls, respectively.

763 The expression of ToxN$_{Pa}$ at the respective time points of infection is shown in the lower panel

764 using Western Blot; C indicates the 11 kDa SdhE-FLAG protein used as a loading and size

36

765   control (41). (B) S1-nuclease assay targeting ToxI$_{Pa}$ for the infection with the escape phage

766   ΦM1-O. The assay was done as in (A).

767

768   FIG 3 Toxicity of the ΦM1 escape locus products. (A) The escape locus of ΦM1 as per Fig. 1B.

769   The positions of the ΦM1 escape phage mutations are shown by red vertical lines, labelled with

770   the parent phage. The scale is in base pairs. (B) Specific regions of the phage genomes,

771   designated by the length of the line that corresponds to the genomic locus shown in (A), were

772   cloned into pBAD30 to make nine different constructs. Blue dotted lines in (A) reflect the

773   construct boundaries in (B). The figure is drawn to scale. (C) Expression of ΦM1 wt and ΦM1-B

774   escape loci in Pba. Strains of Pba containing either a ToxIN$_{Pa}$ or ToxIN$_{Pa}$-FS plasmid (pTRB125

775   or pTRB126), together with a phage construct (or pBAD30 vector control) were tested for

776   toxicity. (D) A range of construct 7 plasmids was tested for toxicity in Pba. The escape phage

777   constructs were all reduced for toxicity. Error bars show the standard deviation in triplicate data.

778

779   FIG 4 Co-immunoprecipitation of M1-23, M1-O-23 and UvrA. (A), and (B) show co-

780   immunoprecipitation experiments with wild type M1-23 and UvrA. In (A) M1-23-6His was used

781   as the bait and attached to a Ni+ column with UvrA-FLAG passed through. In (B) the reciprocal

782   experiment was performed with UvrA-6His used as the bait and M1-23-FLAG was passed

783   through. (C), and (D) show the same co-immunoprecipitation experiments using M1-O-23

784   instead of M1-23. In (C) M1-O-23 was used as the bait and in (D) UvrA-6His was used as bait.

785

786 **Tables**

TABLE 1 Bacterial strains and bacteriophages used in this study

Bacteria	Genotype/ Characteristics	Source
E. coli β2163	F⁻ RP4-2-Tc::Mu *dapA* ::(*erm-pir*), Km^R	(57)
E. coli DH5α	F⁻ *endA1 glnV44 thi-1 recA1 relA1 gyrA96 deoR nupG purB20* φ80d*lacZ*ΔM15 Δ(*lacZYA-argF*)U169, *hsdR17*(r$_K$⁻m$_K$⁺), λ⁻	Gibco/BRL
E. coli ER2566	F⁻ λ- *fhuA2* [*lon*] *ompT lacZ*::T7 gene 1 *gal sulA11* Δ(*mcrC-mrr*)114::*IS10* R(*mcr-73*::miniTn*10*-TetS)2 R(*zgb*-210::Tn*10*)(TetS) *endA1* [*dcm*]	NEB
E. coli W3100	F⁻ λ- *rph-1* INV(*rrhD, rrhE*)	(58)
Pectobacterium atrosepticum SCRI1043	Wild type strain	(31)

Phages	Characteristics	Source
ΦM1	Podoviridae, propagated on wt SCRI1043	(30)
ΦM1-A	ToxIN$_{Pa}$-escape mutant of ΦM1	(29)
ΦM1-B	ToxIN$_{Pa}$-escape mutant of ΦM1	(29)
ΦM1-C	ToxIN$_{Pa}$-escape mutant of ΦM1	(29)
ΦM1-D	ToxIN$_{Pa}$-escape mutant of ΦM1	(29)
ΦM1-O	ToxIN$_{Pa}$-escape mutant of ΦM1	This study
ΦM1-V	ToxIN$_{Pa}$-escape mutant of ΦM1	This study
ΦM1-W	ToxIN$_{Pa}$-escape mutant of ΦM1	This study
ΦM1-X	ToxIN$_{Pa}$-escape mutant of ΦM1	This study
ΦM1-Y	ToxIN$_{Pa}$-escape mutant of ΦM1	This study
ΦM1-Z	ToxIN$_{Pa}$-escape mutant of ΦM1	This study
ΦM1-Q	ToxIN$_{Pa}$-escape mutant of ΦM1	This study
ΦM1-E1 to E49	ToxIN$_{Pa}$-escape mutant of ΦM1	This study
ΦM1-U1	ToxIN$_{Pa}$-escape mutant of ΦM1 on UvrA mutant	This study
ΦM1-U2	ToxIN$_{Pa}$-escape mutant of ΦM1 on UvrA mutant	This study
ΦM1-U4	ToxIN$_{Pa}$-escape mutant of ΦM1 on UvrA mutant	This study
ΦM1-U5	ToxIN$_{Pa}$-escape mutant of ΦM1 on UvrA mutant	This study
ΦM1-U6	ToxIN$_{Pa}$-escape mutant of ΦM1 on UvrA mutant	This study
ΦM1-U7	ToxIN$_{Pa}$-escape mutant of ΦM1 on UvrA mutant	This study
ΦM1-U8	ToxIN$_{Pa}$-escape mutant of ΦM1 on UvrA mutant	This study
ΦM1-U9	ToxIN$_{Pa}$-escape mutant of ΦM1 on UvrA mutant	This study
ΦM1-U10	ToxIN$_{Pa}$-escape mutant of ΦM1 on UvrA mutant	This study
ΦM1-PL2	TenpIN$_{Pl}$-escape mutant of ΦM1	This study

787

TABLE 2 Primers used in this study

Primer	Sequence (5'-3')	Description	Restriction site
KDOI	TTTTGGATCCGTTTTATCGACATTGTGAACC	*toxIN* locus	*Bam*HI
PF147	GTATCTAGAGTAGTCGCCTCTTTTACTTTATTAC	*toxI*	*Xba*I
PF217	TTGTATACTTAAGTTATTGACTCTATAGCTCAG	ToxI amplification for S1-nuclease protection assay	*Hin*dIII
PF218	TTGACTATGTAGTCGCCTCTTTTACTTTATTTCGAACCTCGGACCTGCG	ToxI amplification for S1-nuclease protection assay	*Drd*I
TRB37	CCGGCATATGAAATTCTACACTATATCAAGC	Used for ToxIN CBD	*Nde*I
TRB38	GTGGTTGCTCTTCCGCACTCGCCTTCTTCCGTAT	Used for ToxIN CBD	*Sap*I
TRB107	TTGAATTCTGCGCAAGCAACTGGTGCACC	ΦM1 sequencing primer	*Eco*RI
TRB108	TTAAGCTTCTTGAATCTGTACTCACCG	ΦM1 sequencing primer	*Hin*dIII
TRB111	TTGAATTCCTGTAGGAGCGTGGAATGC	ΦM1 escape locus	*Eco*RI
TRB115	TTGAATTCCAGGGGTGTTACCTACTCC	ΦM1 sequencing primer	*Eco*RI
TRB116	TTAAGCTTGTAACTGTGCAGTGATACC	ΦM1 sequencing primer	*Hin*dIII
TRB117	TTGAATTCCCTACAATGCCCCAGATGC	ΦM1 escape locus	*Eco*RI
TRB118	TTAAGCTTACGGTCGTACTTGGCTTCG	ΦM1 escape locus	*Hin*dIII
TRB125	TTAAGCTTCTAATCCTACGCCTTGTGC	ΦM1 escape locus	*Hin*dIII
TRB126	TTGAATTCAAGGTGGATGCAACTCGGG	ΦM1 escape locus	*Eco*RI
TRB127	TTAAGCTTCTCTACATCATCCAACATC	ΦM1 escape locus	*Hin*dIII
TRB128	TTGAATTCGAGCTGCGTGATGAGTTCC	ΦM1 escape locus	*Eco*RI
TRB129	TTGAATTCGCTTACCCGATTATATCC	ΦM1 escape locus	*Eco*RI
TRB130	TTGAATTCCCAATTTAAAATTAATGA	ΦM1 escape locus	*Eco*RI
TRB134	TTAAGCTTATTACTTGTCATCGTCGTCCTTGTAGTCTCCTAGGTACCCCATCTGG	ΦM1 construct 7/ORF23 FLAG	*Hin*dIII
TRB135	TTAAGCTTAGTGATGGTGATGGTGATGTCCTCCTAGGTACCCCATCTGG	ΦM1 construct 7/ORF23-6His	*Hin*dIII
TRB332	TTAAGCTTATTACTTGTCATCGTCGTCCTTGTAGTCTCCCAGCATCGGCTTAAGGAAGCG	*uvrA*-FLAG	*Hin*dIII
TRB337	ATTAGGATCCGATAAGATCGAAGTTCG	*uvrA* primer	*Bam*HI
TRB338	ATTAAAGCTTTTACAGCATCGGCTTAAG	*uvrA* primer	*Hin*dIII
UvrA dnF	TTTATTCCGGGAAGTGTGTGAATTTAAATTAGCGAGAGGCCAAATCATG	Fwd, 500bp downstream of *uvrA*	*Swa*I
UvrA dnR	TTATCAGAATTCCTGCCGTGCAGGCAGTTCAG	Rev, 500bp downstream of *uvrA*	*Eco*RI
UvrA upF	TTATCATCTAGATTGCAGTGCGCCTTCGATG	Fwd, 500bp upstream of *uvrA*	*Xba*I
UvrA upR	CATGATTTGGCCTCTCGCTAATTTAAATTCACACACTTCCCGGAATAAA	Rev, 500bp upstream of *uvrA*	*Swa*I

788

39

TABLE 3 Plasmids used in this study

Name	Description	Construction	Template	Resistance
pACYC184	Cloning vector	(59)	-	Cm
pBR322	*E. coli* cloning vector	NEB	-	Ap, Tc
pFR2	*Photorhabdus luminescens* TT01 full TenpIN$_{Pl}$ locus	(23)	pBR322	Ap
pKNG-uvrA	UvrA marker exchange construct	UvrA upF, UvrA upR, UvrA dnF, UvrA dnR	pKNG101	Tc, Kan
pKNG101-Tc^R	Marker exchange suicide vector	(60)	-	Tc
pMAT7	SdhE-FLAG expression vector	(41)	pBAD30	Ap
pMJ4	toxI$_{Pa}$, ToxN$_{Pa}$-FLAG with native promoter in pBR322	(29)	pBR322	Ap
pQE80L	Protein expression vector	Qiagen	-	Ap
pRW50	Promoterless LacZ	(49)	-	Tc
pTA46	ToxIN$_{Pa}$ with native promoter	(29)	pBR322	Ap
pTA104	ToxIN$_{Pa}$ promoter	(22)	pRW50	Tc
pTA110	In vitro transcription vector for antisense ToxI$_{Pa}$ RNA	PF217, PF218	pBSII SK$^-$	Ap
pTRB18-KP14	ToxI$_{Pa}$ containing	KDO1, PF147	pACYC184	Cm, Tt
pTRB14	ToxN$_{Pa}$ CBD	TRB37, TRB38	pTA46	Ap
pTRB113	ΦM1 wt construct 3	TRB126+TRB118	pBAD30	Ap, glu
pTRB114	ΦM1 wt construct 4	TRB117, TRB127	pBAD30	Ap, glu
pTRB115	ΦM1 wt construct 5	TRB126, TRB125	pBAD30	Ap, glu
pTRB116	ΦM1 wt construct 6	TRB128, TRB118	pBAD30	Ap, glu
pTRB121	ΦM1-B construct 2	TRB117, TRB125	pBAD30	Ap, glu
pTRB123	ΦM1-B construct 4	TRB117, TRB127	pBAD30	Ap, glu
pTRB124	ΦM1-B construct 5	TRB126, TRB125	pBAD30	Ap, glu`
pTRB133	ΦM1 wt construct 7	TRB111, TRB125	pBAD30	Ap, glu
pTRB134	ΦM1 wt construct 8	TRB129, TRB125	pBAD30	Ap, glu
pTRB135	ΦM1 wt construct 9	TRB130, TRB125	pBAD30	Ap, glu
pTRB136	ΦM1-A construct 7	TRB111, TRB125	pBAD30	Ap, glu
pTRB139	ΦM1-B construct 7	TRB111, TRB125	pBAD30	Ap, glu
pTRB140	ΦM1-B construct 8	TRB129, TRB125	pBAD30	Ap, glu
pTRB141	ΦM1-B construct 9	TRB130, TRB125	pBAD30	Ap, glu
pTRB148	ΦM1 wt construct 7-FLAG	TRB111, TRB134	pBAD30	Ap, glu
pTRB151	ΦM1-O construct 7-FLAG	TRB111, TRB134	pBAD30	Ap, glu
pTRB153	ΦM1-W construct 7-FLAG	TRB111, TRB134	pBAD30	Ap, glu
pTRB154	ΦM1-Y construct 7-FLAG	TRB111, TRB134	pBAD30	Ap, glu
pTRB155	ΦM1-D construct 7	TRB111, TRB125	pBAD30	Ap, glu
pTRB156	ΦM1-O construct 7	TRB111, TRB125	pBAD30	Ap, glu
pTRB157	ΦM1-V construct 7	TRB111, TRB125	pBAD30	Ap, glu
pTRB158	ΦM1-W construct 7	TRB111, TRB125	pBAD30	Ap, glu
pTRB159	ΦM1-Y construct 7	TRB111, TRB125	pBAD30	Ap, glu
pTRB160	ΦM1 wt LacZ fusion construct	TRB117, TRB127	pRW50	Tc
pTRB161	ΦM1 wt LacZ fusion construct	TRB111, TRB127	pRW50	Tc
pTRB162	ΦM1 wt LacZ fusion construct	TRB126, TRB127	pRW50	Tc
pTRB163	ΦM1-O LacZ fusion construct	TRB117, TRB125	pRW50	Tc
pTRB164	ΦM1 wt LacZ fusion construct	TRB117, TRB125	pRW50	Tc
pTRB189	ΦM1-23-6His	TRB111, TRB135	pQE-80L	Ap
pTRB190	ΦM1-O-23-6His	TRB111, TRB135	pQE-80L	Ap
pTRB300	UvrA-FLAG	TRB330, TRB332	pBAD33	Cm, glu
pTRB301	UvrA-6His	TRB337, TRB338	pQE-80L	Ap

789

TABLE 4 Summary of ΦM1 escape mutations and effects on reading frames

Phage	Date of isolation	Mutation relative to ΦM1 wt	Effect on forward reading frames[a]		
			F1	F2	F3
ΦM1-A	Mar 2007	15416 A to C	Y to S	T to P	No change
ΦM1-B	Mar 2007	15292 C to T	R to STOP	No change	P to L
ΦM1-C	Mar 2007	15170 T to C	M to T	STOP to S	No change
ΦM1-D	Mar 2007	15410 T to C	M to T	W to R	No change
ΦM1-O	Jun 2009	15407 A to C	Q to P	No change	No change
ΦM1-V	May 2009	15415 T to G	Y to D	No change	V to G
ΦM1-W	May 2009	15398 A to T	D to V	M to L	STOP to C
ΦM1-X	May 2009	15288 AA to A	FS to STOP after 9 aa (wild type F1 continues *phiM1-23*)	FS causing Q to H and STOP after 3 aa (wild type F2 stops after 9 aa)	FS causing N to T and shift of ORF1 into ORF2 (wild type F3 stops after 3 aa)
ΦM1-Y	May 2009	15397 G to A	D to N	No change	No change
ΦM1-Z	May 2009	15416 A to G (cf M1-A)	Y to C	T to A	No change

[a] 'FS', frameshift; 'aa', amino acid

790

TABLE 5 EOPs against $ToxIN_{Pa}$ and $TenpIN_{Pl}$ Type III TA systems

Phage	EOP vs $ToxIN_{Pa}$	EOP vs $TenpIN_{Pl}$	Escape selected on
ΦM1 wt	1.3×10^{-5}	1.1×10^{-2}	-
ΦS61	$<3.2 \times 10^{-9}$	0.9	-
ΦTE	1.0×10^{-8}	0.7	-
ΦM1-O	1.0	1.0	$ToxIN_{Pa}$
ΦM1-PL2	0.9	0.9	$TenpIN_{Pl}$

791

A

B
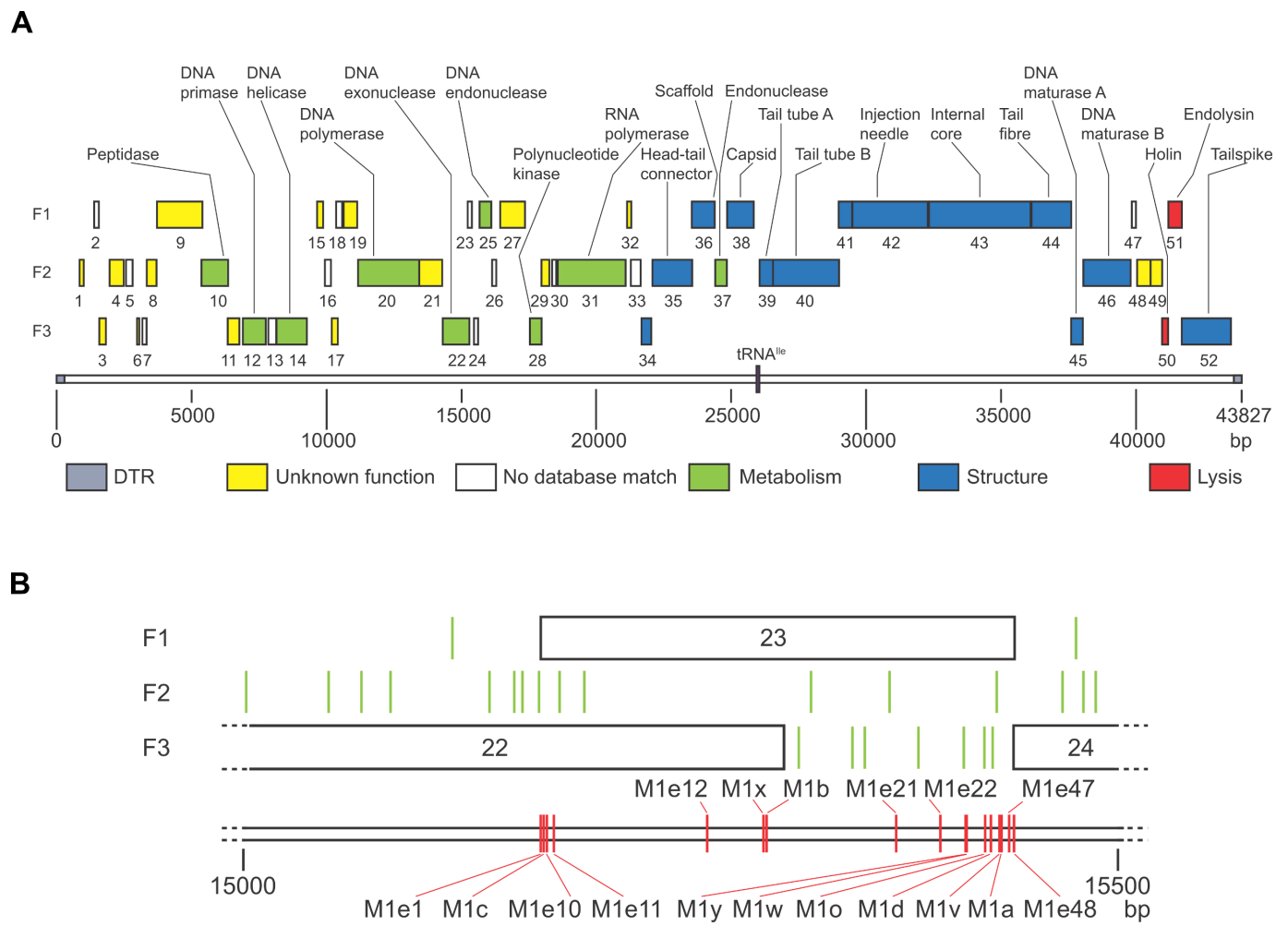

FIG 1 Genomic map of ΦM1 wild type and its escape locus.
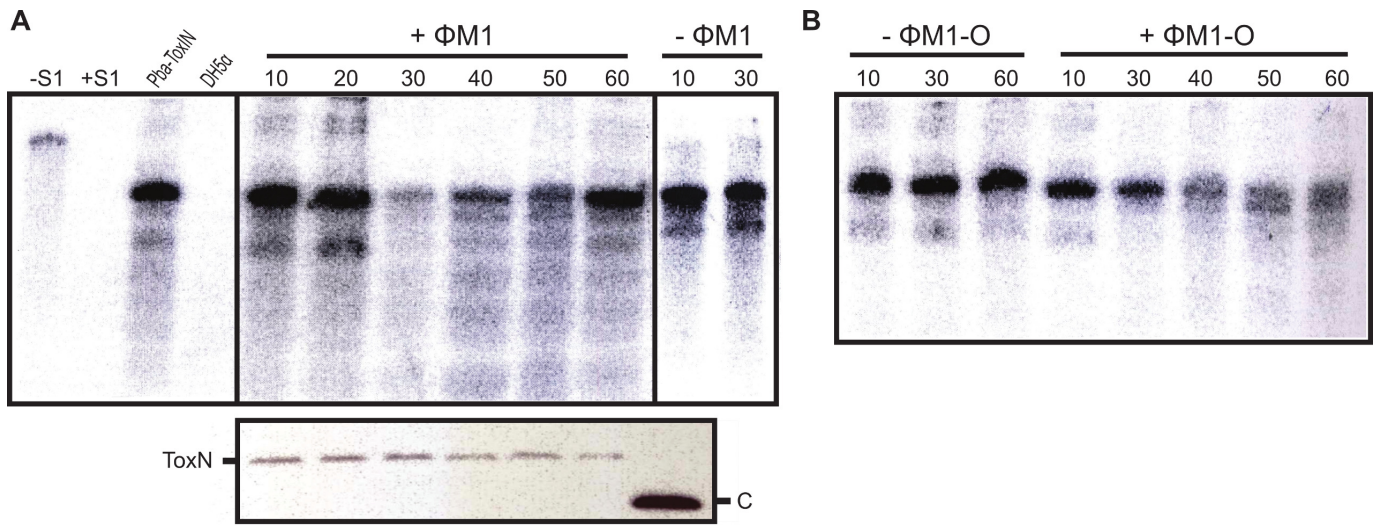
FIG 2 ToxI$_{Pa}$ levels are affected during phage infection.

FIG 3 Toxicity of the ΦM1 escape locus products.

A   M1-23-6His + UvrA-FLAG

	FT	Wash	E1	E2	E3	
Bait						His
Prey						FLAG

B   UvrA-6His + M1-23-FLAG

	FT	Wash	E1	E2	E3	
Bait						His
Prey						FLAG

C   M1-O-23-6His + UvrA-FLAG

	FT	Wash	E1	E2	E3	
Bait						His
Prey						FLAG

D   UvrA-6His + M1-O-23-FLAG

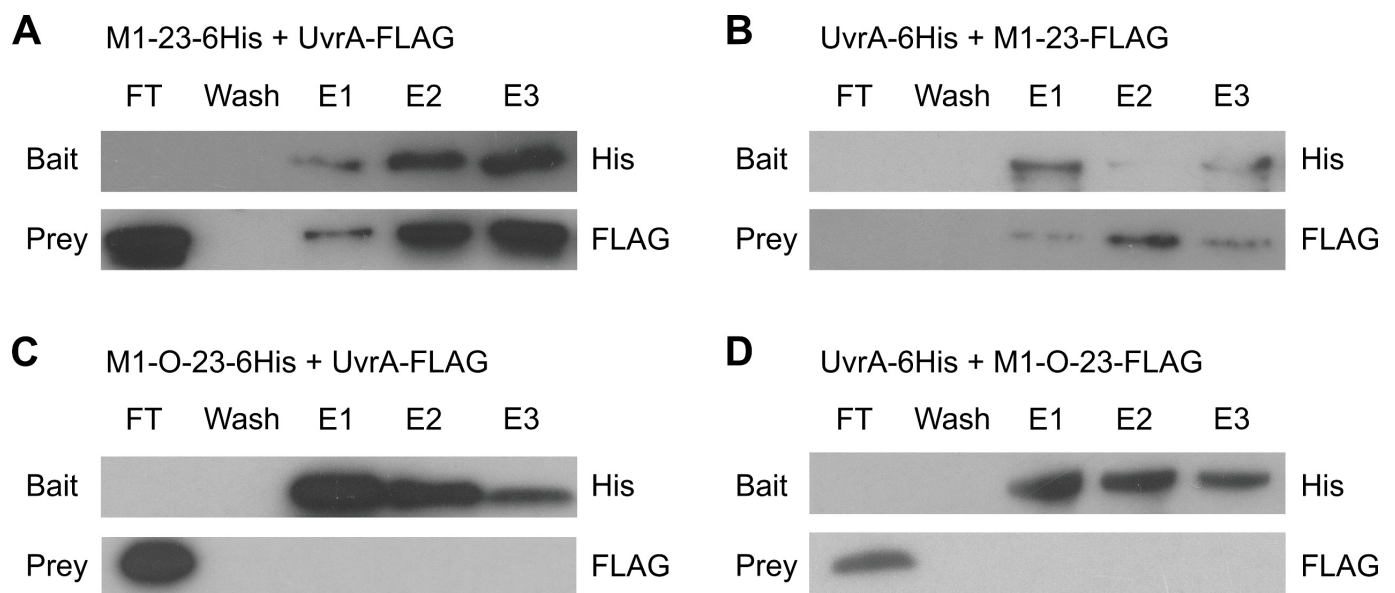|	FT	Wash	E1	E2	E3	
Bait						His
Prey						FLAG

FIG 4 Co-immunoprecipitation of M1-23, M1-O-23 and UvrA.